

DOI: 10.1002/cplu.201300212

Synthesis of Light-Induced Expandable Photoresponsive Polymeric Nanoparticles for Triggered Release

Zhen Wang, Peng Wang, and XinJing Tang*^[a]

High stability of drug-delivery nanocarriers during blood circulation is critical for effective drug delivery and low systematic toxicity, although destabilization of these nanocarriers is required for efficient release when they reach target sites. To develop efficient polymeric nanocarriers, we intended to synthesize and characterize a group of cross-linked, light-induced, expandable, polymeric nanoparticles through miniemulsion polymerization. These synthesized nanoparticles were stable in aqueous solutions, although light irradiation led to particle un-

caging and further particle expansion up to 315-fold in volume. This resulted in the efficient release of the encapsulated contents in aqueous solutions and three cell lines (HeLa, RAW264.7, and MCF-7). Selective triggered release was also successfully achieved with spatial resolution in cell monolayers. In addition, curcumin encapsulation and photoregulation of its release were realized. Further cell viability of encapsulated curcumin was successfully achieved with light activation.

Introduction

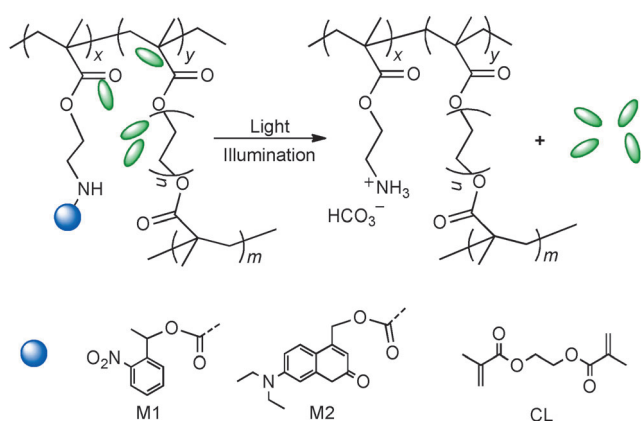
Many materials, such as lipids, carbohydrates, hydroxy acid polymers, dendrimers, and diblock copolymers, have been applied to form micro- and nanoparticles for applications in drug-delivery systems owing to their easy manipulation and chemical modifications.^[1,2] These kinds of polymeric particles are being intensively studied as drug capsules to increase drug solubility and stability, enhance pharmacokinetics, and minimize side effects. Although great improvements for drug delivery with these nanocarriers have been achieved, it is highly desirable to control the release of encapsulated substances to reach high enough drug concentrations and to mediate the effective therapeutic response through an external stimulus. Several triggering events, such as chemical, thermal, electrical, magnetic, biological, and photochemical methods, have been widely applied.^[3,4] However, most events based on these mechanisms require variations in the internal environments, which lead to limited spatiotemporal control of delivery. Among these stimuli, light stands out as a clean and noninvasive one, and has the potential to overcome the above-mentioned limitations owing to the possibility of remote control and manual manipulation of payload release at a specific time, position, and concentration.^[5–8]

Different photosensitive polymeric particle systems have been designed and reported in the literature, and may be divided into the following categories: 1) photoinduced structural changes that lead to destabilization of micelles by photoisomerization (azobenzene, spiropyran, etc)^[9–16] and photodissoci-

ation (*o*-nitrobenzyl, 4-hydroxymethyl coumarin derivatives, etc);^[17–22] 2) photoinduced segmentation of photolabile polymers caused the dissociation of polymers into small fragments through direct photocleavage of the polymer backbone or self-immolation based on the quinone–methide moiety.^[23–26] Both kinds of polymers have shown good capabilities to self-assemble into micelles for target encapsulation and photoinduced release of encapsulated targets. However, these self-assembled micelles may suffer dissociation below their critical micelle concentrations (CMCs), especially in blood vessels. Thus, increasing the stability of polymeric particles is critical for further *in vivo* applications. Cross-linked polymers show high stability as drug nanocarriers.^[27] Several photolabile cross linkers (CLs) have been designed and synthesized. We recently developed a photocleavable CL by using 1-(2-nitrophenyl)ethane-1,2-diol as the photolabile moiety, which was converted into the bismethyl acrylate for cross linking of the internal core of block copolymers.^[28] Further Nile red encapsulation and photo-triggered release were realized. The groups of Anseth and Kasko synthesized photosensitive PEGylated (PEG = polyethylene glycol) CLs with *o*-nitrobenzyl moieties at both terminals and further used these linkers to prepare photosensitive hydrogels for live cell encapsulation and release.^[29,30] Instead of photosensitive CLs, photolabile cross-linked nanocarriers can also be prepared by the application of photolabile subunits and non-photolabile CLs. Anseth et al. applied photolabile peptide subunits to synthesize click-based hydrogel and realize photoreversible patterning of biomolecules for cell adherence.^[29] Herein, we focus on cross-linked photolabile nanocarriers that can be used for the full release of encapsulated substances upon light activation. Previously, an acid-sensitive polymeric particle with 2,4,6-trimethoxybenzaldehyde-protected tris(hydroxymethyl)ethane and a CL (1,4-*O*-methacryloylhydroquinone) achieved acid-induced expandable particles for full release.^[31] Inspired by this study, we intended to design

[a] Z. Wang, P. Wang, Prof. Dr. X. Tang
State Key Laboratory of Natural and Biomimetic Drugs
School of Pharmaceutical Sciences, Peking University
No. 38 Xueyuan Rd., Beijing 100191 (P. R. China)
Fax: (+86) 10-82805635
E-mail: xinjingt@bjmu.edu.cn

 Supporting information for this article is available on the WWW under <http://dx.doi.org/10.1002/cplu.201300212>.



Scheme 1. Above: Strategy for controllable release from light-induced expandable nanoparticles (eNPs). Below: Structures of photolabile monomers (M1 and M2 for eNP1 and eNP2, respectively), and CL for particles synthesized through miniemulsion polymerization.

a series of photosensitive expandable particles for nanocarriers with photolabile monomers, as indicated in Scheme 1.

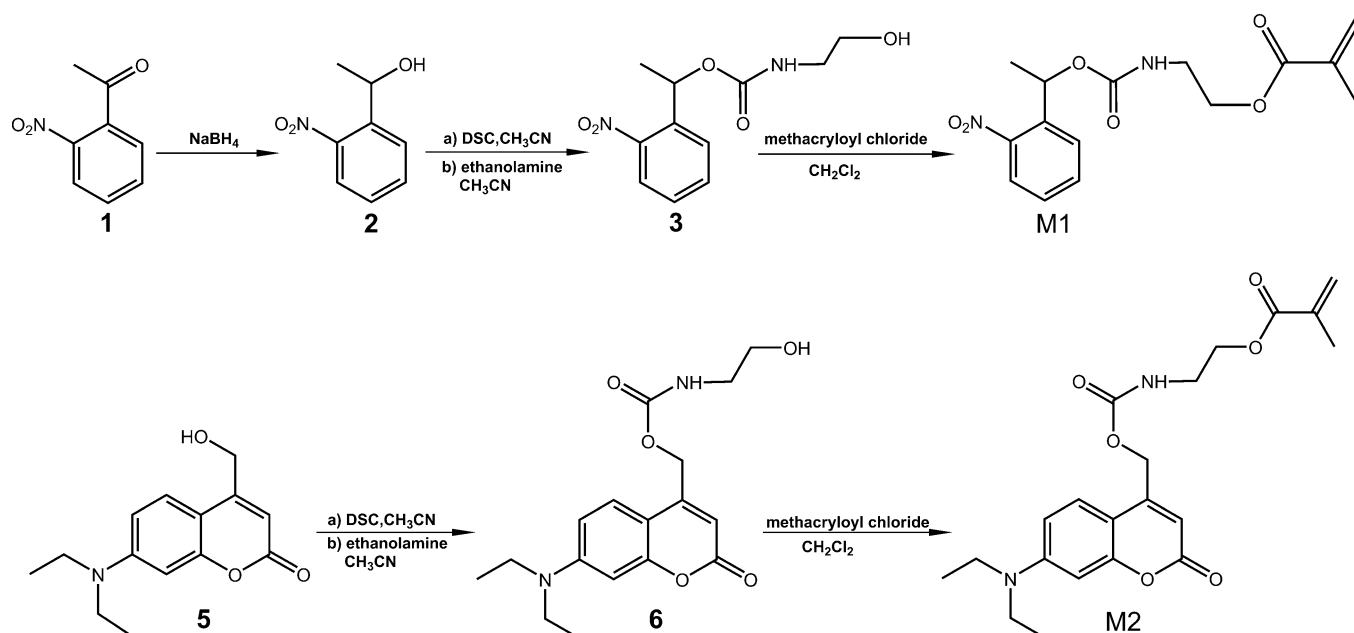
Results and Discussion

Synthesis and characterization of light-induced expandable nanoparticles

To develop such photoresponsive nanoparticles, we first prepared hydrophobic methacrylate monomers (M1 and M2 for eNP1 and eNP2, respectively; Scheme 2). The photolabile moieties of 1-(2-nitrophenyl)ethanol (**2**) and 7-diethylamino-4-hydroxymethylcoumarin (**5**) were synthesized according to literature reports.^[17,32] These two moieties were then converted into *N*-hydroxysuccinimide (NHS) esters and the obtained intermediates could react with aminoethanol to form the corre-

sponding carbamates and mask amine groups. We further esterified the obtained intermediates (**3** and **6**) with methacryloyl chloride to give the photolabile monomers (M1 and M2). At the same time, we also synthesized a photolabile monomer (Ma) and a nonphotolabile monomer (Mc) by direct esterification of **2** and benzyl ethanol with methacryloyl chloride.^[32] With these monomers in hand, we performed the syntheses of polymeric particles through miniemulsion polymerization with the addition of CL (ethylene glycol dimethacrylate) and initiator (azodiisobutyronitrile (AIBN)), according to reported methods.^[31,33,34]

The synthesized particles were not soluble in organic solvents, including DMSO, even though they could be dispersed in deuterated water, so it was not possible to obtain NMR spectra of particles or to perform gel permeation chromatography (GPC). The synthesized nanoparticles were then characterized by dynamic light scattering (DLS), SEM, and UV/Vis and IR spectroscopy (see Figures S1–4 in the Supporting Information). Table 1 lists the diameters of the synthesized nanoparticles with the encapsulation of different substances through DLS (Cumulant method) by using the Zetasizer Nana-ZS instrument from Malvern Instruments at 25 °C. For blank and substance-encapsulated nanoparticles, the diameters were all around 80–130 nm. Interestingly, when the particles (eNP1 and eNP2) with photolabile M1 and M2 were irradiated with light, the particle sizes dramatically increased in aqueous solutions (Figure 1 and Figure S3 in the Supporting Information). Light-induced swelling ratios (LISRs) of these photoresponsive nanoparticles with different encapsulated substances were up to about 315-fold in volume in comparison to those of photolabile (NPc-CL-10%, 1.01) and non-photoresponsive (NPc-CL-10%, 0.99) nanoparticles in aqueous solutions (Table 1). The size expansion of the nanoparticles may be due to the formation of carbon dioxide,^[35] which associates with amine instead of leaking out of



Scheme 2. Synthetic route to photolabile monomers M1 (above) and M2 (below). DSC = *N,N'*-disuccinimidyl carbonate.

	No UV		UV		LISR
	Particle size [nm] (pdi)	Zeta potential [mV]	Particle size [nm] (pdi)	Zeta potential [mV]	$(d_{UV}/d_{noUV})^3$
eNP1-blk-10%	128.7 (0.112)	-18.7	768.9 (0.284)	+46.4	213.2
eNP1-coumarin6-10%	130.9 (0.084)	-25.5	708.1 (0.223)	+32.1	158.3
eNP1-FDA-10%	125.4 (0.140)	-18.0	853.0 (0.263)	+33.8	314.7
eNP1-curcumin-10%	134.2 (0.127)	-38.8	631.0 (0.191)	+26.8	104.0
eNP2-blk-10%	99.7 (0.177)	-18.0	624.5 (0.174)	+33.3	246.0
eNP2-FDA-10%	119.7 (0.212)	-27.0	771.8 (0.115)	+18.9	268.1
NPa-blk-10% ^[b]	112.9 (0.164)	-32.3	113.3 (0.142)	-34.2	1.01
NPC-blk-10% ^[b]	85.2 (0.238)	-34.2	85.1 (0.200)	-33.8	0.99

[a] blk refers to no encapsulation; FDA refers to fluorescein diacetate; 10% refers to the mole percentage of CL (ethylene glycol dimethacrylate) based on the monomers. [b] Control nanoparticles (photolabile; NPa-blk-10%; nonphotolabile: NPC-blk-10%). See Figure S3 in the Supporting Information for the monomer structures.

the nanoparticles upon light activation of the eNPs. The reaction between amine and CO₂ with the involvement of water further solubilizes the internal core of eNPs. This observation is similar to a previous report on CO₂-sensitive polymers.^[36] In addition, the zeta potentials of these nanoparticles were also investigated (Figure 1 and Figure S3 in the Supporting Informa-

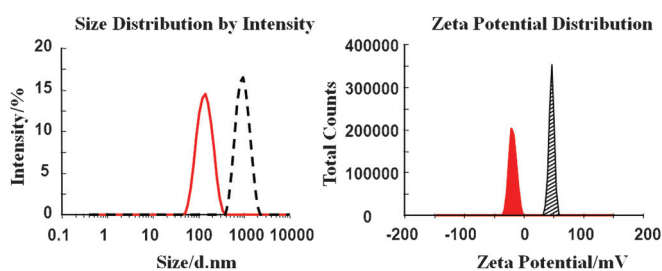


Figure 1. Particle size variation of diameters and zeta potential changes of eNP1-blk-10% before (red) and after (black) light irradiation.

tion). As listed in Table 1, the zeta potentials of eNP1 and eNP2 with the encapsulation of different substances were photo-switched from negative (-18.0 to -38.8) to positive charges (+18.9 to +46.4), while there were almost no charge variations for either photosensitive NPa or nonphotosensitive NPC. The dramatic changes in particle charge further indicated the uncaging of photolabile particles (eNP1 and eNP2) and the release of the amine moiety.

To evaluate the time dependence of the photocleavage of nanoparticles, an aqueous solution of eNP1-blk-10% was irradiated with $\lambda = 365$ nm UV light. The UV/Vis absorbance spectra of the particle solution were measured with different irradiation times. We observed the appearance of a new absorbance peak at $\lambda = 310$ nm, which belonged to the cleaved product, *o*-nitrosophenoacetone.^[37-39] By monitoring the absorbance at $\lambda = 310$ nm, we observed no further increase in the UV/Vis spectra after light irradiation for 20 minutes, which confirmed the maximum conversion of photocleavage. However, this

method does not allow the evaluation of photocleavage of a solution of eNP2-blk-10% particles because of the limited change in UV/Vis absorbance before and after light irradiation. In addition to blank particles, we also determined the in vitro releasing kinetics of coumarin 6 from coumarin 6 loaded nanoparticles (eNP1-coumarin6-10%) by UV/Vis spectra. The maximum release efficiency was close to completeness in 150 s, according to the measurement of precipitated coumarin 6 after UV irradiation (Fig-

ure S5 in the Supporting Information). In comparison to the data for the photocleavage of eNP1-blk-10%, faster release of coumarin 6 from nanoparticles indicated that it was not required for complete photocleavage of caging groups to reach the full release of encapsulated substances in nanoparticles.

We also performed IR measurements on eNP1 and eNP2 nanoparticles before and after light irradiation. For eNP1 particles, the absorption at $\tilde{\nu} = 1527.8$ cm⁻¹ was assigned to the C-NO₂ band, which disappeared with light irradiation. This observation was consistent with previous reports,^[32,37,39] and confirmed photocleavage of the *o*-nitrobenzyl moiety and release of the amine moiety. However, for eNP2 particles, the IR absorption of C=O of the carbamate was buried in that of the absorption for the C=O skeleton and light irradiation did not induce clear changes in the C=O absorption in the IR spectra. Instead, we observed a slightly shifted IR absorption peak, as shown in Figure S1 in the Supporting Information.

Photoresponsive behavior of light-induced expandable nanoparticles in solution and in cells

Coumarin 6, a hydrophobic fluorescence dye, was used as a model to evaluate photocontrolled release in aqueous solution. The dye shows strong fluorescence in the hydrophobic core of the nanoparticles and loses its emission when released in aqueous solution, owing to low solubility. Coumarin 6 was encapsulated in the core of the nanoparticles (eNP-coumarin6-10%) when particles were synthesized through miniemulsion polymerization with photolabile monomer M1. We measured the fluorescence spectra of a solution of eNP-coumarin6-10% with an excitation wavelength of $\lambda = 460$ nm. As shown in Figure 2, the particle solution emitted strong fluorescence when coumarin 6 was excited at $\lambda = 460$ nm before photoactivation. However, a dramatic decrease in fluorescence intensity was observed upon light irradiation. Fluorescence intensity of 200 $\mu\text{g mL}^{-1}$ of eNP-coumarin6-10% decreased about 85% with 5 minutes irradiation. This result indicated photoswitching of the hydrophobic environment of the internal core of the nanoparticle and release of coumarin 6. A plot of fluorescence intensity of an aqueous solution of eNP-coumarin6-10% versus

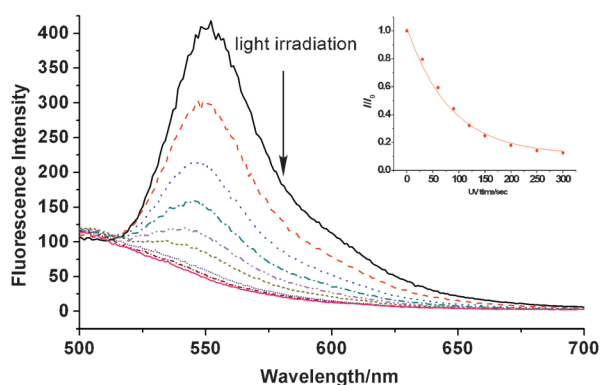


Figure 2. Fluorescence spectra of eNP1-coumarin6-10% upon light irradiation ($\lambda = 365$ nm, 11 mW cm^{-2}) at an excitation wavelength of $\lambda = 460$ nm. The inset shows the normalized fluorescence intensity at $\lambda = 553$ nm versus irradiation time.

irradiation time is given as an insert in Figure 2. By fitting the data with Equation (1), we obtained the characteristic time, τ (96.9 s), at which the fluorescence intensity decreased to 36.8% ($1/e$):

$$I/I_0 = (I/I_0)_m + [1 - (I/I_0)_m] \exp(-t/\tau) \quad (1)$$

For eNP2 nanoparticles, we directly measured the fluorescence spectra of the particle solutions owing to the inherent fluorescence properties of the coumarin moiety. A strong fluorescence emission of **5** in the hydrophobic core of eNP2-blk-10% particles was observed, as expected. However, light irradiation disrupted the hydrophobic properties of the core of the particle, which led to a decrease in fluorescence intensity (Figure S6 in the Supporting Information). However, the maximum decrease in fluorescence intensity was about 40% of its initial value after irradiation for 400 s and no further change was observed with longer irradiation. This is probably because **5** has a higher solubility in aqueous solution than that of coumarin 6 and still has some fluorescence emission, even in aqueous solution.

Nanoparticles (eNP1-coumarin6-10%) were then tested for uptake by three different cell lines (RAW264.7, HeLa, and MCF-7). As illustrated in Figure S7A in the Supporting Information, these three kinds of cells can take up nanoparticles that light up the cells. We also quantified the uptake of the nanoparticles by using cell flow cytometry for HeLa cells with or without the incubation of eNP1-coumarin6-10%. Results shown in Figure S7B in the Supporting Information clearly demonstrate the efficient uptake of eNP1-coumarin6-10% particles by the cells. However, light irradiation did not induce detectable variation in the fluorescence intensity of the cells because coumarin 6 released could also interact with hydrophobic proteins or membranes to show strong fluorescence emission instead of precipitation in the cells, as indicated in Figure S7 in the Supporting Information for cell uptake of eNP1-coumarin6-10% and free coumarin 6.

To further demonstrate the triggered release of encapsulated substances in cells, FDA was chosen because FDA itself is

nonfluorescent, however, upon uptake by cells, intracellular esterases hydrolyze the acetate groups to produce a highly fluorescent product (fluorescein). Although FDA-loaded nanoparticles were taken up by cells, FDA was trapped in the hydrophobic core of the particles and could not be hydrolyzed by esterases. However, once the internal hydrophobic core of the particles was damaged through light irradiation, FDA was quickly released from the internal core of the particles and converted into highly fluorescent fluorescein after hydrolysis. All three kinds of cells were incubated with eNP1-FDA-10% ($62.5 \mu\text{g mL}^{-1}$) for 8 hours and then were thoroughly washed with phosphate-buffered saline (PBS). The uptake of nanoparticles (eNP1-FDA-10%) and triggered release of FDA in cells were visualized directly by fluorescence microscopy. Figure 3a shows fluorescent images of three cell lines under different conditions. As expected, light irradiation lit up all three kinds of cells, which indicated uptake and triggered release of FDA in the cells. We further quantified the fluorescence intensity of the triggered release of FDA before and after light irradiation by measuring the fluorescence intensity of all three kinds of cells in 96-well plates by using a microplate reader. Light irradiation for 15 minutes led to 6–8-fold increase in fluorescence intensity for all three cell lines that took up eNP1-FDA-10% nanoparticles (Figure 3b). Because light and eNP1-FDA-10% themselves did not lead to strong fluorescence emission, eNP1-FDA-10% must have been photochemically uncaged and FDA was released. We also evaluated another kind of photosensitive nanoparticle (eNP2) with a photolabile coumarinyl moiety instead of a 2-nitrobenzyl moiety according to a similar procedure. The triggered release of FDA from eNP2-FDA-10% was also successfully achieved in RAW264.7 and HeLa cells with a large increase in fluorescence from hydrolyzed FDA (Figure S8 in the Supporting Information) of 11- and 7-fold for RAW264.7 and HeLa cells, respectively. Because several reports have demonstrated that the coumarinyl group can be uncaged through two-photon excitation,^[17,25] we expected that substances encapsulated in these coumarinyl-caged polymeric nanoparticles would also be released by two-photon activation.

Light-induced patterned release in cells

With these particles in place, we further tested their applicability for making a simple pattern of FDA release in cell monolayers. The ability to do this has the potential to make significant contributions to the study of drug release with the spacing and timing for a specific cell. We used the same nanoparticles (eNP1-FDA-10% and eNP2-FDA-10%) as those described above. Cells were first plated in 35 mm glass-bottomed dishes and further incubated with these FDA-loaded nanoparticles for 12 hours and then thoroughly washed with PBS. Half of each examined dish was masked from direct light exposure by sticking the mask as close to the cells as possible. Because the light source was not collimated, nor a point source, we still observed some light leakage at the edge of the mask. The resulting patterned images are shown in Figure 4 and Figure S9 in the Supporting Information. For both RAW264.7 and HeLa cells, the irradiated cells lit up, while the other half of the cells

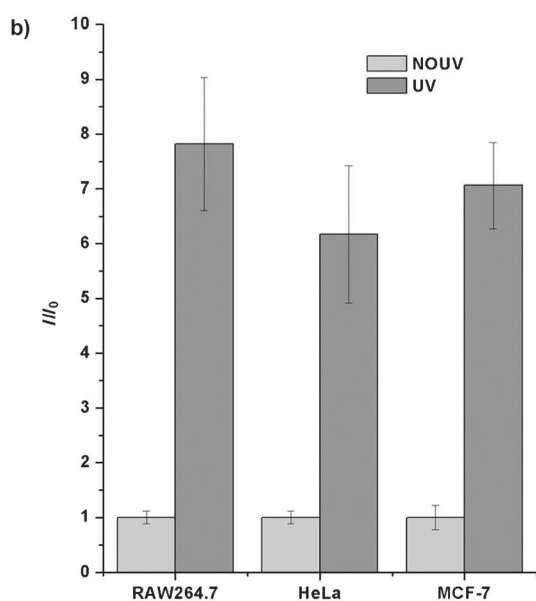
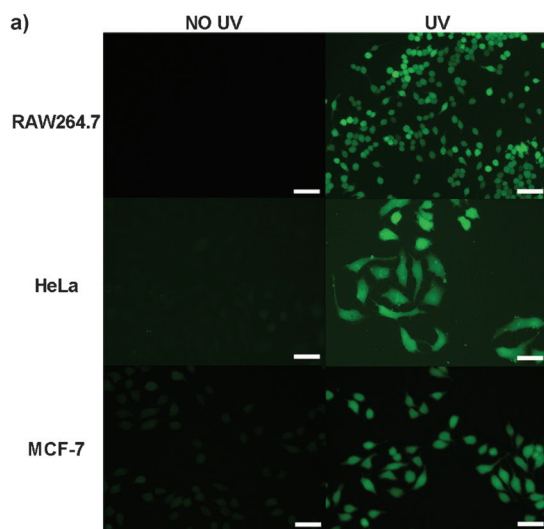


Figure 3. a) Fluorescence images of RAW264.7, HeLa, and MCF-7 cells incubated with eNP1-FDA-10% for 8 h followed by light irradiation for 15 min and imaging. b) Enhancement ratios of the fluorescence intensity of three cell lines after incubation with eNP1-FDA-10%. The fluorescence intensity was measured before and after light activation by using a microplate reader. The concentration of particle solutions was $62.5 \mu\text{g mL}^{-1}$ (scale bar = $50 \mu\text{m}$).

in the same dishes did not show fluorescence emission when they were covered by the masks. All of these results indicate that these photoresponsive eNPs are promising for use in the photoregulation of drug release with spatial resolution.

Drug loading and phototriggered release in HeLa cells

Instead of model chromophores, curcumin, which is a component of Indian ayurvedic medicine, was chosen for further encapsulation and triggered release from the nanoparticles described above (Figure S10 in the Supporting Information). Previously, *in vitro* and animal studies suggested that curcumin had promising applications in the treatment of different dis-

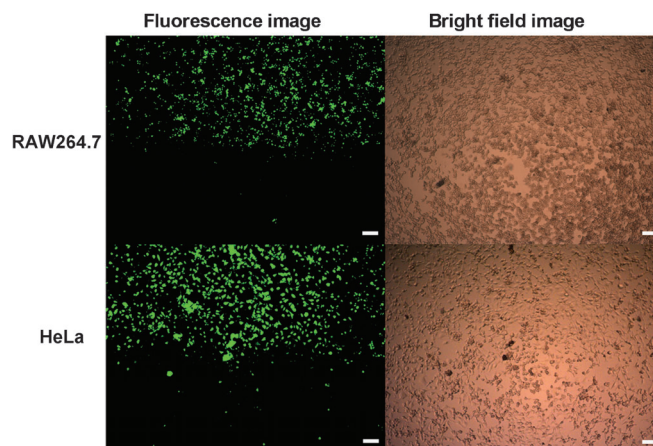


Figure 4. Patterning of the phototriggered release of FDA with photoresponsive eNP2-FDA-10% nanoparticles. In each image, the top half of the cells were irradiated and showed fluorescence emission (scale bar = $100 \mu\text{m}$).

eases and viruses.^[40] Because of its limited solubility and instability, curcumin is difficult for the body to absorb. Nanocurcumin (a polymer nanoparticle encapsulated formulation of curcumin) has the potential to bypass many of the disadvantages associated with free curcumin.^[41] With a similar procedure of miniemulsion polymerization as that mentioned above, we solubilized curcumin through its encapsulation into the hydrophobic core of eNP1-curcumin-10%. Similar to coumarin 6 or FDA-loaded nanoparticles, we also evaluated the triggered release of eNP1-curcumin-10% in aqueous solution. Curcumin itself has almost no fluorescence emission in solution. In hydrophobic environment it emits fluorescence at $\lambda = 505 \text{ nm}$ with excitation at $\lambda = 420 \text{ nm}$. We measured the fluorescence spectra of an aqueous solution of eNP1-curcumin-10% at different irradiation times and monitored the intensity of the peak at $\lambda = 505 \text{ nm}$. Figure S11 in the Supporting Information shows that the fluorescence intensity of a solution of curcumin-loaded nanoparticles decreased to 20% of the initial fluorescence intensity within 600 s of light irradiation; this indicated the efficient triggered release of curcumin from the internal core of the nanoparticles in aqueous solutions.

Triggered release of curcumin from eNP1-curcumin-10% was further evaluated in HeLa cells. First, the toxicity of these nanoparticles was studied by incubating cells with varying concentrations of these blank particles for 48 hours. No clear signs of toxicity were found up to $250 \mu\text{g mL}^{-1}$ of eNP1-blk-10% with or without exposure to light for 15 min and further incubation for 48 hours (Figure S12 in the Supporting Information). Free curcumin showed cell toxicity of $\text{IC}_{50} = 4.2 \mu\text{g mL}^{-1}$ without irradiation and $3.6 \mu\text{g mL}^{-1}$ with light irradiation for 15 min, as determined by a sulforhodamine B (SRB) assay. The results showed that light had little effect on the cytotoxicity of curcumin to HeLa cells (Figure S13 in the Supporting Information). However, if curcumin was loaded into photoresponsive nanoparticles, it was trapped inside the hydrophobic core and did not leak out. The entrapment efficiency of curcumin by the particles was determined to be 71.5% by UV/Vis absorbance at $\lambda = 428 \text{ nm}$. According to the IC_{50} value of curcumin for HeLa

cells, we chose four different concentrations of aqueous solutions of eNP1-curcumin-10% particle (100, 150, 200, and 250 $\mu\text{g mL}^{-1}$, which corresponded to curcumin concentrations of 3.14, 4.71, 6.28, and 7.85 $\mu\text{g mL}^{-1}$, respectively) for the evaluation of cell viability. As shown in Figure 5, the cell viability was almost unchanged for cells treated with up to 250 $\mu\text{g mL}^{-1}$ of eNP1-curcumin-10%, whereas light irradiation of cells treated with eNP1-curcumin-10% particles clearly triggered cell death of up to 85%. Because there was no clear light-induced cytotoxicity of eNP1-blk-10% (Figure S12 in the Supporting Information), the dramatic variation in cytotoxicity was assumed to be from curcumin released upon light activation.

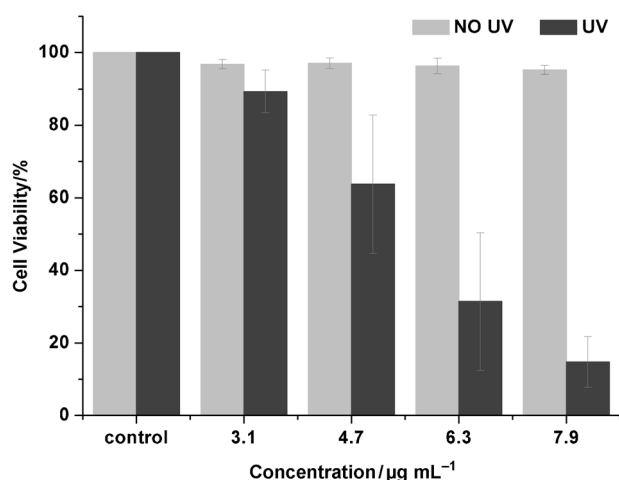


Figure 5. The viability of HeLa cells exposed to different concentrations of eNP1-curcumin-10% nanoparticles (with corresponding curcumin concentrations of 3.14, 4.71, 6.28 and 7.85 $\mu\text{g mL}^{-1}$, respectively). The UV exposure time was 15 min.

Conclusion

We synthesized a series of cross-linked, light-induced, expandable, polymeric particles with different photolabile monomers (nitrobenzyl and coumarinyl) through miniemulsion polymerization. The synthesized particles were stable in aqueous solutions, however, light irradiation caused the release of the amine moiety from internal hydrophobic core, which led to the swelling of nanoparticles with LISR values of up to 315-fold in volume and the efficient release of the encapsulated contents. The release efficiency reached 85% based on the fluorescence intensity variations of coumarin 6. Uptake and triggered release of the encapsulated substances from different cell lines was observed with FDA-loaded nanoparticles. Selective triggered release of cell monolayers was also successfully achieved. In addition, encapsulation of bioactive curcumin in photoresponsive nanoparticles and light-triggered release of curcumin were realized. Further cell experiments showed that curcumin released from a 250 $\mu\text{g mL}^{-1}$ solution of eNP1-curcumin-10% particles caused cell death of up to 85% with 15 minutes irradiation. This new light-triggered expandable particle system

may afford a new option for the photocontrollable treatment of cancers and other diseases with spatiotemporal resolution.

Experimental Section

General methods

All commercially solvents and reagents were used without further purification except as noted below. Tetrahydrofuran, triethylamine (TEA), and xylene were purified by distillation over CaH_2 . 7-*N,N*-Diethylamino-4-methylcoumarin, SeO_2 , DSC, and coumarin 6 were purchased from J&K Chemicals. Methacryloyl chloride was purchased from TCI Shanghai. Ethanolamine, ethylene glycol dimethacrylate (CL) and trichloroacetic acid (TCA) were purchased from Alfa Aesar. FDA was purchased from Alfa Aesar and stored at -20°C . SRB was purchased from Sigma Aldrich (St. Louis, MO, USA). Hexadecane (HD) was purchased from Haltermann in Germany. SDS and Tris base were purchased from Beijing Dingguo Biotechnology Co. AIBN was purchased from Shanghai trial four Hervey Chemical Co.

^1H and ^{13}C NMR spectra were recorded on a Bruker AVANCEIII 400 MHz NMR spectrometer. Reported chemical shifts (ppm) were relative to CDCl_3 or $[\text{D}_6]\text{DMSO}$ and coupling constants were reported in Hz. The diameters of nanoparticles were determined by DLS at 25°C with a Zetasizer Nana-ZS instrument from Malvern Instruments. FTIR spectra were measured by using a Nicolet NEXUS-670 FTIR spectrometer. UV/Vis spectra were recorded on a DU800 UV/Vis spectrophotometer (Beckman, USA). Fluorescence spectra were obtained by using a Cary Eclipse fluorometer (Varian, USA). SEM (Hitachi S-4300) was used to observe the particles: typically one drop of diluted nanoparticle solution was cast on silicon wafer, and dried at 37°C . FDA release in cells was detected with a FlexStation 3 Molecular Devices instrument. Cell uptake was observed with an inverted fluorescence microscope (OLYMPUS, IX81). Patterned cell experiments were acquired with a Zeiss Upright fluorescence microscope (Axio Imager A2). A B-100SP lamp (UVP, LLC) was used as the light resource for irradiation ($\lambda = 365\text{ nm}$, 11 mW cm^{-2}).

Synthesis

1-(2-nitrophenyl)ethanol (2): Compound 2 was synthesized according to a literature procedure with minor modifications.^[28] An aqueous solution of NaBH_4 (34.4 mL, 10%) was added dropwise to the solution of 1 (5 g, 30 mmol) in 1,4-dioxane (30 mL) at 0°C . The mixture was stirred in an ice cold bath for 1 h and at room temperature for an additional 30 min. Excess NaBH_4 was then quenched with acetone (20 mL). After removal of the solvents, the residue was extracted with ethyl acetate, and the organic layer was dried over anhydrous sodium sulfate. When ethyl acetate was removed, the light-yellow oil obtained was used in the next step without further purification (98%). ^1H NMR (400 MHz, CDCl_3): $\delta = 7.91$ (d, $J = 8.1\text{ Hz}$, 1H), 7.85 (d, $J = 7.8\text{ Hz}$, 1H), 7.66 (t, $J = 7.7\text{ Hz}$, 1H), 7.42 (t, $J = 7.7\text{ Hz}$, 1H), 5.43 (q, $J = 6.4\text{ Hz}$, 1H), 1.58 ppm (d, $J = 6.4\text{ Hz}$, 3H); ^{13}C NMR (101 MHz, CDCl_3): $\delta = 147.9$, 141.0, 133.7, 128.2, 127.7, 124.4, 65.6, 24.3 ppm.

1-(2-nitrophenyl)ethyl (2-hydroxyethyl)carbamate (3): DSC (2.7 g, 10.5 mmol) was added to a solution of 2 (1.1 g, 6.6 mmol) in CH_3CN (60 mL), followed by the addition of TEA (2.7 mL, 18.6 mmol). The mixture was stirred overnight at room temperature. Ethanolamine (1 g, 16.4 mmol) was then added and the solution was stirred for another 6 h at room temperature. Solvents

were evaporated to dryness and the residue was dissolved in CH_2Cl_2 , washed thoroughly with a saturated solution of NaHCO_3 , and then washed with brine. The organic layer was dried over anhydrous sodium sulfate. After removal of CH_2Cl_2 , the residue was purified by column chromatography over silica gel (petroleum ether/ethyl acetate=2:1) to give **3** as a light-yellow oil (77.8%). ^1H NMR (400 MHz, CDCl_3): δ =7.91 (d, J =8.2 Hz, 1H), 7.64–7.62 (t, J =2.3 Hz, 3.6 Hz, 2H), 7.45–7.39 (m, 1H), 6.24 (q, J =6.4 Hz, 1H), 5.41 (s, 1H), 3.63 (t, J =4.9 Hz, 2H), 3.26 (t, J =5.2 Hz, 2H), 2.56 (s, 1H), 1.62 ppm (d, J =6.4 Hz, 3H); ^{13}C NMR (101 MHz, CDCl_3): δ =161.1, 152.6, 143.5, 138.6, 133.2, 132.2, 129.3, 73.8, 66.8, 48.3, 27.2 ppm; MS: m/z : 277.21 [$M+\text{Na}$] $^+$.

2-((1-(2-nitrophenyl)ethoxy)carbonyl)amino)ethyl methacrylate (M1): Compound **3** (0.8 g, 3.2 mmol) and dry TEA (1.4 mL, 9.6 mmol) were dissolved in dry CH_2Cl_2 (20.0 mL). The mixture was then purged with nitrogen and allowed to stir in an ice cold bath for 5 min. Methacryloyl chloride (0.53 mL, 5.5 mmol) was slowly added over a period of 10 min. The reaction mixture was then warmed to room temperature and stirred overnight. After the reaction was complete, the mixture was then washed three times with a saturated solution of NaHCO_3 and once with brine. The resulting organic phase was dried over anhydrous sodium sulfate and then concentrated in vacuo. The residue was purified by column chromatography over silica gel (petroleum ether/ethyl acetate=6:2) to give **M1** monomer as a light-yellow oil (88.7%). ^1H NMR (400 MHz, CDCl_3): δ =7.93 (d, J =8.1 Hz, 1H), 7.61 (d, J =4.1 Hz, 2H), 7.44–7.38 (m, 1H), 6.25 (q, J =6.5 Hz, 1H), 6.10 (s, 1H), 5.59 (d, J =1.4 Hz, 1H), 5.02 (s, 1H), 4.19 (t, J =5.2 Hz, 2H), 3.49–3.40 (m, 2H), 1.93 (s, 3H), 1.62 ppm (d, J =6.5 Hz, 3H); ^{13}C NMR (101 MHz, CDCl_3): δ =172.3, 160.4, 152.5, 143.6, 140.9, 138.6, 133.2, 132.1, 131.1, 129.3, 73.6, 68.5, 45.0, 27.1, 23.2 ppm; MS: m/z : 345.20 [$M+\text{Na}$] $^+$.

7-Diethylamino-4-hydroxymethylcoumarin (5): A solution of SeO_2 (414 mg, 3.73 mmol) and **4** (570 mg, 2.63 mmol) in xylene (50 mL) was heated at reflux under a nitrogen atmosphere. After 18 h, the mixture was filtered and concentrated under the reduced pressure. The dark-brown residual oil was dissolved in ethanol (50 mL), followed by the addition of NaBH_4 (414 mg, 3.73 mmol). The reaction mixture was stirred for 4 h at room temperature, and then carefully hydrolyzed with 1 M HCl. The reaction solution was concentrated under reduced pressure to remove ethanol. The resulting mixture was extracted with CH_2Cl_2 and washed twice with a saturated solution of NaHCO_3 . The organic phase was dried over MgSO_4 and concentrated in vacuo. The resulting oil was purified by column chromatography over silica gel (CH_2Cl_2 /acetone 20:1) to yield **5** as a light-yellow solid (46.2% over two steps). ^1H NMR (400 MHz, CDCl_3): δ =7.30 (d, J =9.0 Hz, 1H), 6.55 (dd, J =8.9, 2.1 Hz, 1H), 6.47 (d, J =2.0 Hz, 1H), 6.27 (s, 1H), 4.82 (d, J =3.6 Hz, 2H), 3.38 (q, J =7.1 Hz, 4H), 1.18 ppm (t, J =7.1 Hz, 6H); ^{13}C NMR (101 MHz, CDCl_3): δ =162.9, 156.1, 155.1, 150.5, 124.4, 108.7, 106.4, 105.3, 97.7, 60.9, 44.8, 12.5 ppm.

7-Diethylamino-4-methylcoumarin-4-yl methyl (2-hydroxyethyl) carbamate (6): DSC (0.65 g, 2.63 mmol) was added to **5** (0.3 g, 1.21 mmol) dissolved in CH_3CN (40 mL), followed by the addition of TEA (0.67 mL, 4.61 mmol). The mixture was stirred overnight at room temperature, then ethanolamine (250 mg, 4.10 mmol) was added, and the reaction solution was stirred for another 6 h. CH_3CN was removed in vacuo, and the residue dissolved in CH_2Cl_2 was washed thoroughly with a saturated solution of NaHCO_3 then brine. The organic layer was dried over anhydrous sodium sulfate. Further purification with column chromatography over silica gel (CH_2Cl_2 /acetone 5:1) gave **6** as a light-yellow solid (42.1%). ^1H NMR (400 MHz, $[\text{D}_6]\text{DMSO}$): δ =7.48–7.43 (m, 1H), 6.69 (d, J =8.5 Hz,

1H), 6.54 (s, 1H), 5.98 (s, 1H), 5.21 (s, 2H), 4.69 (t, J =4.9 Hz, 1H), 3.42 (d, J =6.6 Hz, 6H), 3.09 (d, J =5.6 Hz, 2H), 1.11 ppm (t, J =6.5 Hz, 6H); ^{13}C NMR (101 MHz, $[\text{D}_6]\text{DMSO}$): δ =160.9, 155.8, 155.6, 152.0, 150.5, 125.4, 108.8, 105.3, 104.4, 96.9, 60.9, 59.9, 44.1, 43.2, 12.4 ppm; MS: m/z : 357.23 [$M+\text{Na}$] $^+$.

(7-Diethylamino-4-methylcoumarin-4-ylmethoxycarbonylamino)ethyl methacrylate (M2): Compound **6** (0.13 g, 0.39 mmol) and dry TEA (0.17 mL, 1.17 mmol) were dissolved in dry CH_2Cl_2 (20.0 mL). The solution was then purged with nitrogen and allowed to stir in an ice cold bath for 5 min. Methacryloyl chloride (0.10 mL, 1.04 mmol) was slowly added over a period of 10 min. The reaction mixture was then warmed to room temperature and stirred overnight. The reaction mixture was washed three times with a saturated solution of NaHCO_3 and once with brine. The resulting organic phase was dried over anhydrous sodium sulfate and concentrated in vacuo. The residue was purified by column chromatography over silica gel (CH_2Cl_2 /acetone 20:1) to give **M2** as a light-yellow solid (43.6%). ^1H NMR (400 MHz, CDCl_3): δ =7.30 (d, J =9.0 Hz, 1H), 6.59 (dd, J =8.9, 2.0 Hz, 1H), 6.51 (d, J =2.1 Hz, 1H), 6.12 (d, J =5.9 Hz, 2H), 5.61 (s, 1H), 5.34 (s, 1H), 5.23 (s, 2H), 4.27 (t, J =5.2 Hz, 2H), 3.56 (dd, J =5.6 Hz, 10.9 Hz, 2H), 3.40 (q, J =7.0 Hz, 4H), 1.96 (s, 3H), 1.20 ppm (t, J =7.0 Hz, 6H); ^{13}C NMR (101 MHz, CDCl_3): δ =167.3, 162.0, 156.2, 155.6, 150.5, 150.2, 135.9, 126.3, 124.4, 108.7, 106.1, 97.8, 63.5, 61.9, 44.8, 40.4, 18.3, 12.4 ppm; MS: m/z : 425.27 [$M+\text{Na}$] $^+$.

Nanoparticle Synthesis

Nanoparticles were prepared through miniemulsion polymerization methods.^[31,33,34] In a typical run, monomers (50 mg); ethylene glycol dimethacrylate (CL, 10% mol of the monomers); coumarin **6** (0.5 mg for coumarin **6** loaded particles), FDA (4 mg for FDA-loaded particles), or curcumin (2.1 mg, for curcumin-loaded particles) in acetone (50 μL), 5% AIBN in CH_2Cl_2 (10 μL , w/w), and co-stabilizer HD (3.1 mg) were dissolved in CH_2Cl_2 (500 μL). Distilled water (5 mL) or pH 4 sodium acetate buffer solution (for FDA-loaded particles, FDA is stable at pH 4 at 80 °C) containing sodium dodecyl sulfate (SDS; 5 mg) was first purged by bubbling nitrogen for 10 min, and was then added to the oil phase. The mixture was sonicated in an ice bath for 5 min (JY92-IIN, Ningbo Scientz Biotechnology Co., Ltd, 3 s pulses with 1 s delay) with 80 W of the power. Following sonication, the solution was transferred to a 25 mL sealed container purged with nitrogen. Polymerization was performed at 80 °C in an oil bath for 18 h. After polymerization, the suspension was stirred overnight, which allowed CH_2Cl_2 to evaporate. The aqueous solutions were then dialyzed with a dialysis membrane (8000–14000 g mol^{-1}) against a 1% aqueous solution of DMSO and then with water for 2 days with replacement of dialysis solution every several hours to remove excess surfactant.

Characterization of particles

The mean particle size (diameter) and zeta potential of particles were recorded by using a photon correlation spectroscopy technique in a particle size analyzer (Zetasizer Nano ZS, Malvern Instruments, UK) at 25 °C. The morphological shape of a typical nanoparticle was observed by SEM (Hitachi S-4300). For SEM analysis, the sample was completely dried at 37 °C and coated with gold.

Encapsulation efficiency (EE) of curcumin-loaded particles

The EE of curcumin incorporated in the nanoparticles was determined by dispersing the drug-loaded nanoparticles (0.5 mg) in ethanol and sonication (JK-5200B, Hefei Kinnick Machinery Manufacturing Co., Ltd.) for 12 h to ensure curcumin was dissolved thoroughly, and the precipitated polymer was removed by centrifuging the samples at 30000g for 20 min twice. The concentration of curcumin was then determined by UV/Vis spectroscopy at $\lambda = 428$ nm. The measurements were performed in duplicate. The calculated EE was 71.5% from Equation (2), according to the standard curve (Figure S10 in the Supporting Information). Similar to the method described above, the EE of eNP1-coumarin6-10% was 62.2% by UV/Vis absorbance at $\lambda = 460$ nm, according to the standard curve (Figure S5 in the Supporting Information).

$$\text{Entrapment efficiency (\%)} = \frac{\text{amount of loaded drug (mg)}}{\text{amount of added drug (mg)}} \times 100\% \quad (2)$$

Photodegradation and light-triggered release study

To study the photodegradation of the nanoparticles, a $12.5 \mu\text{g mL}^{-1}$ suspension of particles in a quartz cuvette was irradiated and UV/Vis absorption spectra were recorded after each irradiation. Coumarin 6 and curcumin were used as hydrophobic fluorophores to study the triggered release in solutions and cells. The in vitro release kinetics of coumarin 6 from the particles was determined. Briefly, a $200 \mu\text{g mL}^{-1}$ solution of eNP-coumarin6-10% nanoparticles was irradiated with UV light ($\lambda = 365$ nm, 11 mW cm^{-2}). At predetermined time points, samples were measured by means of a fluorometer with an excitation wavelength of $\lambda = 460$ nm and the emission spectra were recorded from $\lambda = 500$ to 750 nm. For curcumin-loaded nanoparticles (eNP-curcumin-10%), the emission spectra were recorded from $\lambda = 450$ to 700 nm with an excitation wavelength of $\lambda = 420$ nm. All measurements were performed in triplicate.

In addition to light-induced variation of fluorescence intensity, we also quantified the released and precipitated coumarin 6 after light activation, eNP1-coumarin6-10% (samples diluted 25-fold, $200 \mu\text{g mL}^{-1}$) was irradiated at $\lambda = 365$ nm at intervals. Aliquots (400 μL) from a solution of irradiated particles (4.0 mL) were removed at different irradiation times. The aliquots were centrifuged at 1000g for 5 min to separate the precipitated coumarin 6 and dried under vacuum. Then dried coumarin 6 was dissolved in dichloromethane (450 μL) and centrifuged at 30000g for 10 min. The amounts of released coumarin 6 at different irradiated solutions were determined by absorbance at a wavelength of $\lambda = 460$ nm.

Cell culture

Macrophage cell line (RAW264.7) was grown in Dulbecco's modified Eagle cell culture medium (DMEM) containing 10% heat-inactivated fetal bovine serum (FBS), 100 IU mL^{-1} penicillin-streptomycin in an atmosphere of 5% CO_2 and 95% relative humidity. The cells were routinely passaged at 80–95% confluency. Prior to use, cells were harvested by trypsinization (0.125% trypsin/0.05% ethylenediaminetetraacetic acid (EDTA)).

Human uterine cervical cancer cells (HeLa) and MCF-7 were grown at 37 °C in a humidified atmosphere with 5% CO_2 in Roswell Park Memorial Institute (RPMI) medium 1640, supplemented with 10%

FBS and 100 IU mL^{-1} penicillin-streptomycin. The cells were routinely passaged at 80–95% confluency. Prior to use, cells were harvested by trypsinization (0.25% trypsin–0.02% EDTA).

In vitro cellular uptake studies by fluorescence microscopy

The cellular uptake of coumarin 6 loaded nanoparticles was studied by fluorescence microscopy (IX-81, OLYMPUS Co., Tokyo, Japan). Briefly, RAW264.7, HeLa, or MCF-7 cells were seeded into six-well plates at a density of 5×10^4 cells per well and cultured at 37 °C for 12 h, $62.5 \mu\text{g mL}^{-1}$ of coumarin 6 loaded nanoparticles were added. After incubation for 8 h, the culture medium was removed and the cells were rinsed twice with PBS for fluorescence assessment.

FDA-loaded particle uptake and release in cell study

FDA-loaded particles were incubated with RAW264.7 macrophage cells, HeLa, or MCF-7 for 8 h. After incubation, cells were thoroughly washed with PBS and were then irradiated with $\lambda = 365$ nm UV light for 15 min. The images were observed by means of an inverted fluorescence microscope 10 min later, and the fluorescence intensity of cells incubated with FDA-loaded particles either with or without light irradiation were recorded by using a Molecular Devices instrument (FlexStation 3, excitation wavelength 488 nm, emission wavelength 530 nm).

Patterned imaging experiment

For patterned imaging, RAW264.7 (6×10^5) and HeLa cells (2×10^5) were plated in 35 mm glass-bottomed dishes overnight. After the addition of $62.5 \mu\text{g mL}^{-1}$ solutions of eNP1-FDA-10% or eNP1-FDA-10%, the cells were cultured for another 24 h. Cells were washed with PBS twice and refilled with PBS. Then half of the dish was masked. The other half was illuminated for 15 min with an upward-facing light-emitting diode (LED) array (Shenzhen Planck Photoelectric Co., Ltd, $\lambda = 365$ nm, 15 mW cm^{-2}). After 15 min, images were acquired by using a Zeiss upright fluorescence microscope (Axio Imager A2).

Cytotoxicity study on the particles

The cytotoxicity of nanoparticles was evaluated by using an SRB assay. HeLa cells were seeded in 96-well plates at a density of 6×10^4 cells per well. After proliferation for 12 h, cells were treated with various amounts of particles (eNP1-blk-10%; 100 to $250 \mu\text{g mL}^{-1}$) and incubated for 12 h. The cells were divided into two groups ("UV" and "no UV" group). The UV group was irradiated for 15 min. After incubation for another 48 h for both groups, cellular protein was fixed by the addition of 10% TCA (200 μL) at 4 °C for 1 h, the 96-well plates were then washed five times with deionized water and air dried. SRB solution (100 μL ; 4 mg mL^{-1} in 1% acetic acid) was added to each well and the cells were stained for 30 min. Then, SRB solution was removed and the plates were washed five times with 1% acetic acid. After air drying, 10 mM Tris base solution (150 μL) was added to the 96-well plates to solubilize the protein-bound dye on a gyratory shaker for 15 min. Absorbance values were read on a microplate reader (Flexstation 3, Molecular Devices) at a wavelength of $\lambda = 540$ nm.

For cell viability to curcumin, HeLa cells were seeded at a density of 6×10^4 cells mL^{-1} in a 96-well plate and incubated overnight to allow the cells to attach to the surface of the wells. The cells were

then exposed to nanoparticles (eNP1-curcumin-10%) with various concentrations close to the IC_{50} value of curcumin for HeLa cells. After incubation for 12 h, cells treated with eNP1-curcumin-10% were thoroughly washed and cells in the UV group were then irradiated with $\lambda = 365$ nm light for 15 min. After incubation for another 48 h, the cell viability was determined by SRB assay, as described above, and IC_{50} values were calculated based on the percentage of treatment over control. Experiments were repeated three times and data were presented as mean \pm SD.

Acknowledgements

This study is supported by the National Basic Research Program of China (973 Program; grant no. 2013CB933800), the Innovation Team of the Ministry of Education (no. BMU20110263) and the Higher Education Doctoral Fund (20100001120051) of the Ministry of Education of China, and the Program for New Century Excellent Talents in University (NCET-10-0203).

Keywords: curcumins · drug delivery · encapsulation · nanoparticles · photochemistry

- [1] S. K. Sahoo, V. Labhasetwar, *Drug Discovery Today* **2003**, *8*, 1112–1120.
- [2] V. Mohanraj, Y. Chen, *Trop. J. Pharm. Res.* **2006**, *5*, 561–573.
- [3] A. P. Esser-Kahn, S. A. Odom, N. R. Sottos, S. R. White, J. S. Moore, *Macromolecules* **2011**, *44*, 5539–5553.
- [4] M.-H. Li, P. Keller, *Soft Matter* **2009**, *5*, 927–937.
- [5] Y. Zhao, *Macromolecules* **2012**, *45*, 3647–3657.
- [6] N. Fomina, J. Sankaranarayanan, A. Almutairi, *Adv. Drug Delivery Rev.* **2012**, *64*, 1005–1020.
- [7] G. P. Robbins, M. Jimbo, J. Swift, M. J. Therien, D. A. Hammer, I. J. Dmochowski, *J. Am. Chem. Soc.* **2009**, *131*, 3872–3874.
- [8] B. N. P. Kamat, G. P. Robbins, J. Rawson, M. J. Therien, I. J. Dmochowski, D. A. Hammer, *Adv. Funct. Mater.* **2010**, *20*, 2588–2596.
- [9] G. Wang, X. Tong, Y. Zhao, *Macromolecules* **2004**, *37*, 8911–8917.
- [10] C. J. Barrett, J.-i. Mamiya, K. G. Yager, T. Ikeda, *Soft Matter* **2007**, *3*, 1249–1261.
- [11] J. H. Liu, Y. H. Chiu, *J. Polym. Sci. Polym. Chem.* **2010**, *48*, 1142–1148.
- [12] H. Lee, W. Wu, J. K. Oh, L. Mueller, G. Sherwood, L. Petean, T. Kowalewski, K. Matyjaszewski, *Angew. Chem.* **2007**, *119*, 2505–2509; *Angew. Chem. Int. Ed.* **2007**, *46*, 2453–2457.
- [13] E. Mabrouk, D. Cuvelier, F. o. Brochard-Wyart, P. Nassoy, M.-H. Li, *Proc. Natl. Acad. Sci. USA* **2009**, *106*, 7294–7298.
- [14] J. del Barrio, L. Oriol, R. Alcalá, C. Sánchez, *Macromolecules* **2009**, *42*, 5752–5760.
- [15] Q. Jin, G. Liu, X. Liu, J. Ji, *Soft Matter* **2010**, *6*, 5589–5595.
- [16] Y. Liu, C. Yu, H. Jin, B. Jiang, X. Zhu, Y. Zhou, Z. Lu, D. Yan, *J. Am. Chem. Soc.* **2013**, *135*, 4765–4770.
- [17] J. Babin, M. Pelletier, M. Lepage, J.-F. Allard, D. Morris, Y. Zhao, *Angew. Chem.* **2009**, *121*, 3379–3382; *Angew. Chem. Int. Ed.* **2009**, *48*, 3329–3332.
- [18] J. Jiang, X. Tong, Y. Zhao, *J. Am. Chem. Soc.* **2005**, *127*, 8290–8291.
- [19] X. Jiang, C. A. Lavender, J. W. Woodcock, B. Zhao, *Macromolecules* **2008**, *41*, 2632–2643.
- [20] Z. Xie, X. Hu, X. Chen, G. Mo, J. Sun, X. Jing, *Adv. Eng. Mater.* **2009**, *11*, B7–B11.
- [21] B. Yan, J.-C. Boyer, N. R. Branda, Y. Zhao, *J. Am. Chem. Soc.* **2011**, *133*, 19714–19717.
- [22] E. Cabane, V. Malinova, S. Menon, C. G. Palivan, W. Meier, *Soft Matter* **2011**, *7*, 9167–9176.
- [23] N. Fomina, C. McFearin, M. Sermsakdi, O. Edigin, A. Almutairi, *J. Am. Chem. Soc.* **2010**, *132*, 9540–9542.
- [24] N. Fomina, C. L. McFearin, A. Almutairi, *Chem. Commun.* **2012**, *48*, 9138–9140.
- [25] C. de Gracia Lux, C. L. McFearin, S. Joshi-Barr, J. Sankaranarayanan, N. Fomina, A. Almutairi, *ACS Macro Lett.* **2012**, *1*, 922–926.
- [26] N. Fomina, C. L. McFearin, M. Sermsakdi, J. M. Morachis, A. Almutairi, *Macromolecules* **2011**, *44*, 8590–8597.
- [27] S.-F. Chong, J. H. Lee, A. N. Zelikin, F. Caruso, *Langmuir* **2011**, *27*, 1724–1730.
- [28] L. Yu, C. Lv, L. Wu, C. Tung, W. Lv, Z. Li, X. Tang, *Photochem. Photobiol.* **2011**, *87*, 646–652.
- [29] A. M. Kloxin, A. M. Kasko, C. N. Salinas, K. S. Anseth, *Science* **2009**, *324*, 59–63.
- [30] D. R. Griffin, A. M. Kasko, *J. Am. Chem. Soc.* **2012**, *134*, 13103–13107.
- [31] A. P. Griset, J. Walpole, R. Liu, A. Gaffey, Y. L. Colson, M. W. Grinstaff, *J. Am. Chem. Soc.* **2009**, *131*, 2469–2471.
- [32] Z. Wang, L. Yu, C. Lv, P. Wang, Y. Chen, X. Tang, *Photochem. Photobiol.* **2013**, *89*, 552–559.
- [33] K. Landfester, N. Bechthold, F. Tiarks, M. Antonietti, *Macromolecules* **1999**, *32*, 5222–5228.
- [34] F. J. Schork, Y. Luo, W. Smulders, J. P. Russum, A. Butte, K. Fontenot, *Adv. Polym. Sci.* **2005**, *175*, 129–255.
- [35] X. Tang, I. J. Dmochowski, *Org. Lett.* **2005**, *7*, 279–282.
- [36] D. Han, O. Boissiere, S. Kumar, X. Tong, L. Tremblay, Y. Zhao, *Macromolecules* **2012**, *45*, 7440–7445.
- [37] C. Lv, Z. Wang, P. Wang, X. Tang, *Langmuir* **2012**, *28*, 9387–9394.
- [38] F. Yan, L. Chen, Q. Tang, R. Wang, *Bioconjugate Chem.* **2004**, *15*, 1030–1036.
- [39] C. Lv, Z. Wang, P. Wang, X. Tang, *Int. J. Mol. Sci.* **2012**, *13*, 16387–16399.
- [40] P. K. Vemula, J. Li, G. John, *J. Am. Chem. Soc.* **2006**, *128*, 8932–8938.
- [41] S. Bisht, G. Feldmann, S. Soni, R. Ravi, C. Karikar, A. Maitra, A. Maitra, *J. Nanobiotechnol.* **2007**, *5*, 3.

Received: May 28, 2013

Published online on July 16, 2013